Geotechnical and Geophysical Site Characterisation 5 – Lehane, Acosta-Martínez & Kelly (Eds)

Two-Dimensional Non-linear Dynamic Response of a Heap Leach Pad Located in Peru

F.C. Perez
Amec Foster Wheeler Peru

J.D. Ale
Universidad San Ignacio de Loyola, Lima, Peru

ABSTRACT: In this research a dynamic characterization in function of mean stress of share wave velocities and his corresponding maximum shear modulus (V_s, G_{max}) of ROM (run of mine) ore stacking were carried out based on MASW survey. In addition a triaxial compression tests (consolidated undrained, CU of 6" diameter) have been carried out to determine the mechanical properties of the ROM ore stacking of sandstone crushed material. The study has focused on the understanding of the two-dimensional non-linear dynamic response of a heap leach pad located in a higher seismicity Andean region of Peru. This geostructure modeled in Finite Differences Method software (FLAC, Itasca) was subjected to an Operating Basis Earthquake (OBE) obtained from a spectral matching in the time domain (Abrahamson, 1993). A constitutive Mohr-Coulomb Model with stress-level dependent is used to simulate the stress-strain behavior of the ore material. The slope stability and the permanent deformations at the end of this excitation are evaluated. As well as, the development of the deformations during the earthquake are present here in.

1 INTRODUCTION

The current technology of lixiviation process has been widely developed since the last thirty years, becoming this in an efficient method to treat oxidized gold, silver and copper minerals and extract precious metals from small and shallow ore deposits. Important mining operations in regions with a higher seismic activity have the leaching process as their main mineral extraction method. This scenery have generated the necessity for further knowledge in dynamic analysis in order to understand the dynamic response and optimize safely the civil and geotechnical designs of these mining structures. This paper studies a real case of a heap leach facility which the ore stack is composed of quartz-sandstone material.

2 PROPERTIES OF THE QUARTZ-SANDSTONE ORE MATERIAL SPECIMENS

2.1 *Physical Properties and Parameters*

In order to characterize the ROM material was performed a laboratory test program on three samples of quartz-sandstone ore material from a heap leaching project located in the Andean region of Peru. Figure 1 shows the grain-size distribution of the samples analyzed, considering a sample fraction of maximum particle size of 3 inches. The characteristics of these materials, including USCS classification, dry unit weight, and effective Mohr-Coulomb parameters (obtained from triaxial compression tests consolidated undrained TX-CU in 6-inch-diameter samples) are presented in Table 1.

The grain-size distribution of these quartz-sandstone ore materials is very variable, and according to UCSC these samples are classified as: SP-SM, GM, and GP-GM. The Mohr-Coulomb strength parameters determined from the 6" TX-CU tests vary, in terms of effective internal friction angle (ϕ'), from 36.4 to 38.8°. They also vary, in terms of effective cohesion (c), from 7 to 9 kPa.

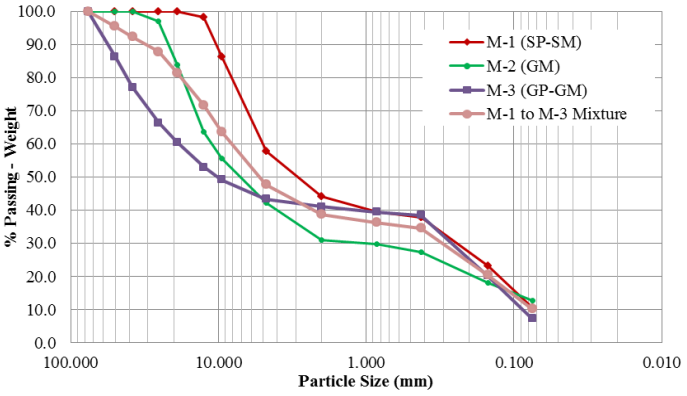

Figure 1. Grain-size distribution of angular quartz-sandstone ore material samples.

Table 1. Mechanical properties of the quartz-sandstone ore material.

Id	UCSC classification	Dry unit weight γ_d (kN/m^3)	Initial confining stresses, σ'_3 (kPa)	c' (kPa)	ϕ' (°)
M-1	SP-SM	17.1	600; 300; 150	7	36.4
M-2	GM	17.7	600; 300; 150	0	38.2
M-3	GP-GM	17.9	600; 300; 150	9	38.8

2.2 *Lithological Characterization*

The specimens tested were composed mainly of quartz-sandstone of fine to medium grain from the Chimu Formation in the northern Andes of Peru. This sedimentary formation is arranged in thick layers (over 0.50 m) and has great strength. It almost always is rough and steep. In some areas one can see the presence of silt-claystones and siltstones, which are sometimes interbedded with coal layers (Navarro et al., 2010). Loose materials from this formation usually have a granular nature with minimal fines content. They are primarily non plastic materials of angular to very angular shape, and with high resistance. Granular materials from the quartz-sandstones of the Chimu Formation are considered as competent material, potentially suitable for use as structural fill, drainage gravel, and rockfill.

2.3 *Multi-channel Analysis of Surface Waves (MASW) Survey*

Were estimated the maximum dynamic shear stress modulus (G_{max}) in *in-situ* conditions, shear-wave (V_s) velocities profiles were extracted from a geophysical investigation, based on a multi-channel analysis of surface waves (MASW) surveying performed on an *in-situ* M-3 sample. The MASW profile obtained from that area is shown in Figure 2.

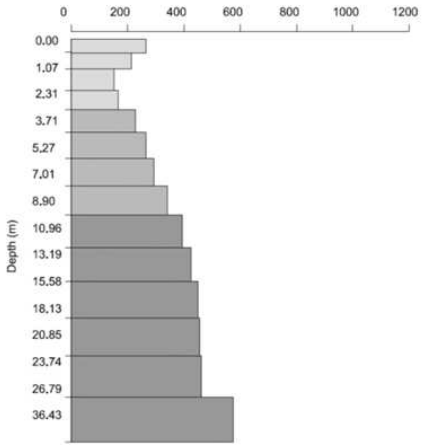

Figure 2. Profile of shear-wave velocity in depth over sample M-3 *in-situ* location.

3 GROUND-MOTION PARAMETERS

3.1 *Seismicity of the Region*

The Peruvian Andes, region where this geostructure is located, were formed as tectonic effect of the subduction of the Nazca Plate under the South American Plate. The rock mass in this region were subjected to strong deformations over 40 million years ago, during a period of intense volcanic activity 15 million years ago. The seismicity of this region is considered as higher, with registered data of about 110 epicenters of earthquakes of 4.0 M_w and epicentral depths <100 km located within 200 km. All historical earthquakes with magnitudes above 6.0 M_w have occurred over 100 km from the site.

3.2 *Earthquake Time History*

For the non-lineal dynamic analysis was selected an input signal considering an Operating Basis Earthquake (OBE), usually defined as the earthquake for which a structure is designed to remain its operational condition, with the damage being readily repairable following the event. Considering that the OBE is likely to occur during the design life of the structure and the seismicity of the region, was selected the seismic event of 5.7 M_w occurred in 01-03-2015 (according with the seismicity of the region), which location is presented in Figure 3.

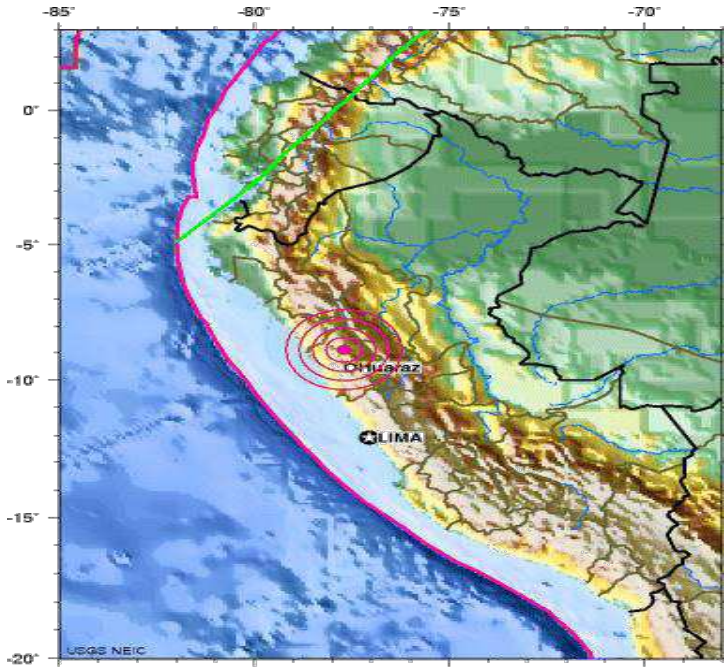

Figure 3. Location of earthquake 5.7 M_w occurred in 01-03-2015 (www.usgs.gov/).

3.3 *Site Response Spectrum for Design*

The design site response spectrum, presented in Figure 4, was previously calculated based on probabilistic methods, having a 2% probability of exceedance in 50 years.

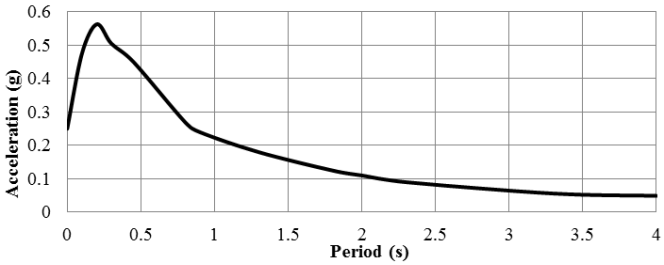

Figure 4. Design response spectrum.

3.4 *Shear Modulus for Granular Soils*

Most available data on maximum shear modulus (G_{max}) has been developed for either sand or gravelly soils. Because most soils have curvilinear stress-strain relationships, it will be appreciated that G_{max} is not constant but is usually expressed as the secant modulus determined for the specific value of shear strain. Seed and Idriss (1970) and Seed et al. (1986) have shown that G_{max} values for gravelly soils are strongly influenced by confining pressure (σ'_m, expressed in Equation 2), strain amplitude (γs), and void ratio (e), finding the relationship in Equation 1 that conveniently related G_{max} and σ'_m.

$$G_{\max} = 21.7 K_{2.\max} P_a \left(\frac{\sigma'_m}{P_a} \right)^{1/2} kPa \qquad (1)$$

$$\sigma'_m = \left(\frac{\sigma'_1 + \sigma'_2 + \sigma' 3}{3} \right) \qquad (2)$$

where $G_{\max}$ = maximum shear modulus, $K_{2.\max}$ = shear modulus at small shear strains (10^{-4}%), σ'_{m} = mean effective confining stress, Pa = atmospheric pressure (100 kPa), and $\sigma'_{1,2,3}$ = maximum, intermediate and minimum effective stresses.

In order to obtain the main effective confining stress, a unit weight at moisture content of 5% was considered for M-3 embankment and at-rest earth pressure coefficient (k_0) of 0.5 was obtained considering the Equation 3 and ν=0.33 from TX-CU in the deformed sample at the end of the test. The $K_{2.\max}$ value presented was obtained from a parabolic function regression in a $\sigma'_m - V_s$ plot presented in Figure 5.

$$\nu = \frac{k_0}{1 + k_0} \qquad (3)$$

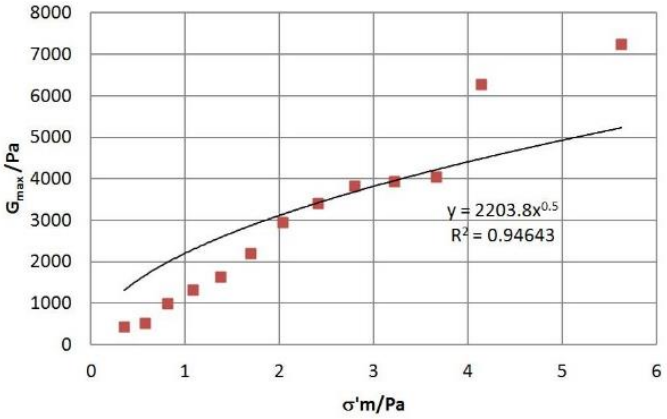

Figure 5. Determination of $K_{2.\max}$.

Where ν = poisson's ratio and k_0 = at-rest earth pressure coefficient.

The $K_{2.\max}$ value is obtained by the division of the x-coefficient of the adjusted parabolic equation in Figure 5 by 21.7 (Equation 1) obtaining a $K_{2.\max}$ = 101.55, as is shown in Table 2.

Table 2. Value of $K_{2.\max}$ in quartz-sandstone ore material.

ID	UCSC classification	MASW Depth (m)	G_{max}	
			$K_{2.\max}$	R^2*
M-3	GP-GM	0-36.43	101.55	0.94643

* R^2 is the adjusted R-squared value of the equation

3.5 *Internal Friction Angle*

The internal friction angles obtained from 6" CU-TX of the quartz-sandstone ore material were evaluated following the method proposed by Barton & Kjaersnly (1981) and expressed in Barton (2008). The estimated parameters used in Equation 4 are listed in Table 3, and are similar with those reported by Leps (1970) for similar frictional materials.

$$\phi = \phi_1 - \Delta\phi \log\left(\frac{\sigma'_3}{P_a} \right) \qquad (4)$$

where ϕ_1 and $\Delta\phi$ = reference friction angle (at $P' = P_a$) and friction angle reduction for every log cycle of stress level increase, respectively.

Table 3. Strength Parameters Used.

ID	UCSC classification	Average dry unit weight γ_d (kN/m^3)	Unit weight γ (kN/m^3)	ϕ (°)	$\Delta\phi$ (°)
M-1 to M-3 Mixture	GP-GM	17.5	19.0	37	5

3.6 *Finite Differences Element Model*

The 140-meter-high model conformed by heap leach stack (80 m high) and basement rock (60 m high) were discretized using a finite-differences grid composed of 35x170 regions in the vertical and horizontal directions, respectively. The special element size (Δl) of zones was 4 m according to Equation 5. The quartz-sandstone ore material was stacked in 1.5H:1V inter-bench slope (of benches of 8 m high and 9 m width) and 2.5H:1V global slope, placed above -3% slope surface of about 520 m over a total model length of 700 m.

$$\Delta l = \frac{\lambda}{8} \qquad (5)$$

where λ = wavelength associated with the highest frequency component that contains appreciable energy of the input wave.

Figure 6 shows the FLAC finite differences model along with the different material zones considered in the analysis and the history control points considered. A built-in Mohr-Coulomb model with stress-level dependent was implemented using the programming language FISH following the Equations 1, 2 and 4, this code was applied to quartz-sandstone ore material in order to obtain the distribution of G_{max} in function of σ'_m and the distribution of effective internal friction angle in function of σ'_3, as is shown in Figure 7 and 8, respectively.

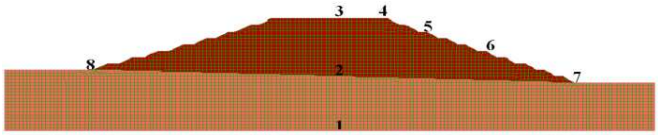

Figure 6. Profile FLAC finite differences model (with history points).

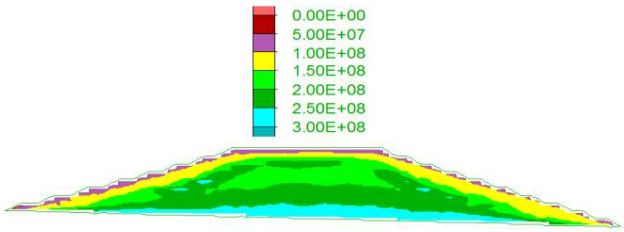

Figure 7. Distribution of G_{max} (Pa) in function of σ'_m

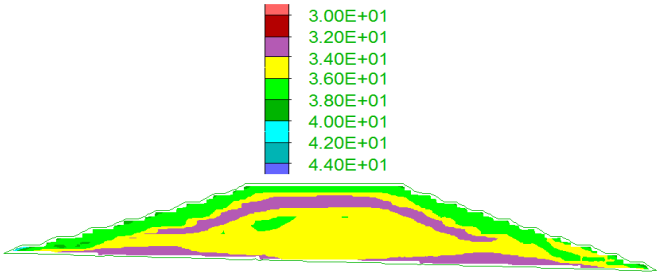

Figure 8. Distribution of effective internal friction angle (°) in function of σ'_3.

3.7 *Spectral Matching*

The time domain matching procedure was used to modify the historic OBE record and match its spectrum to the design spectrum at 5% damping, following the methodology proposed by Abrahamson (1992) and Hancock et al. (2006), Figure 9 present results of the

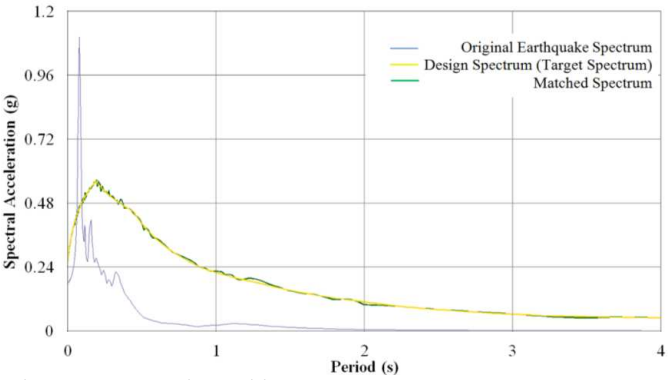

Figure 9. Spectral matching.

matching procedure application. Previously the original time history was corrected by baseline and filtering in order of the maximum frequency of 8 Hz, using the computer program EZ-Frisk (2011). Figure 10 (left) presents the component strong motion compatible with the site response spectrum, used in the dynamic analysis.

4 ANALYSIS RESULTS

4.1 *Acceleration Amplification*

The horizontal acceleration time history computed at the top of the leach pad (history point 3) due to OBE design imposition reached a maximum acceleration of about 0.5g, its value represents about 2 times the peak ground acceleration of the imposed signal (0.25g), as is shown in Figure 10a and 10b.

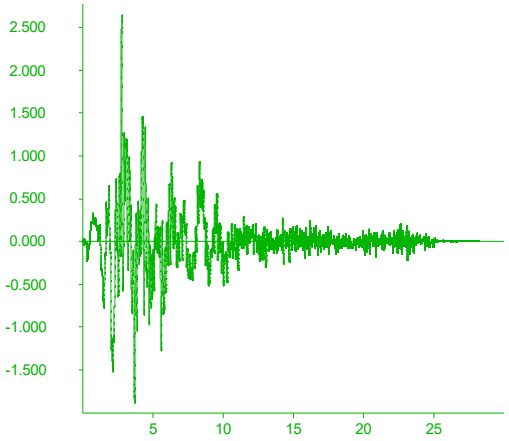

Figure 10a. Acceleration time history at the base of FLAC model a_x (m/s^2) vs t (s).

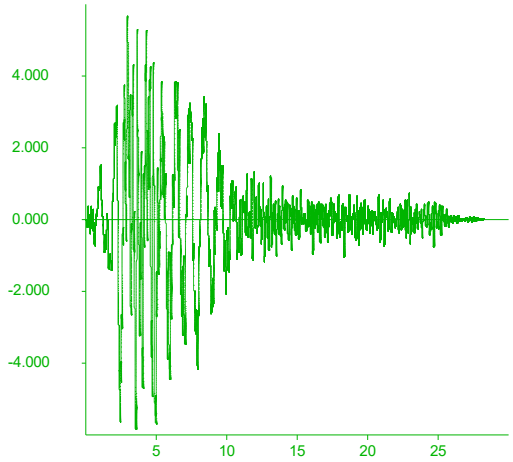

Figure 10b. Acceleration time history at the top of FLAC model a_x (m/s^2) vs t (s).

4.2 *Maximum Permanent Displacements*

Figure 11 and 12 shows the permanent horizontal and permanent displacements contours in the body of the leach pad, respectively, as obtained by applying the input motion at the base of the model. The horizontal displacements reach their maximum values near to the slope of the ore stack in the benches, obtaining deformations of 0.5 m, decreasing in magnitude deepening inside the slope at 0.1 m until null displacements.

The vertical reach their maximum values near to the slope of the ore stack in the benches, obtaining deformations of 0.25 m, decreasing in magnitude deepening inside the slope at 0.05 m until null displacements.

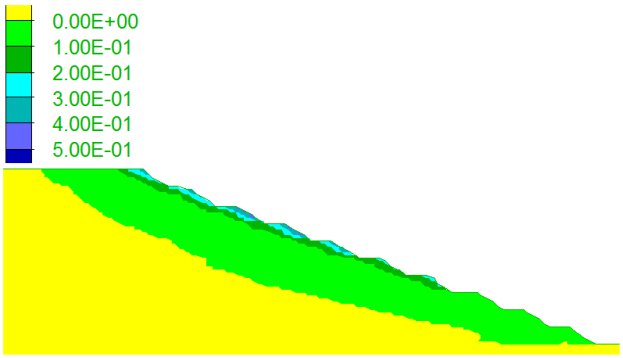

Figure 11. Horizontal displacements in meters.

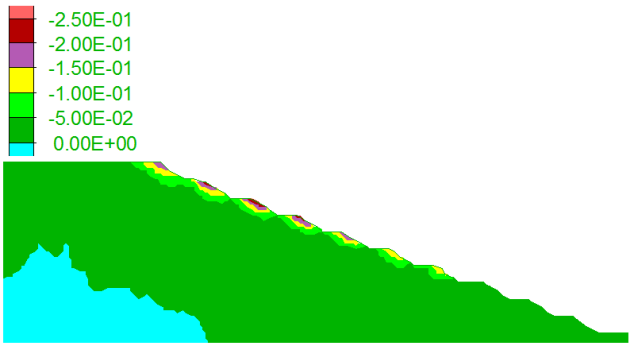

Figure 12. Vertical displacements in meters.

4.3 *Time History Displacement*

Figure 13a and 13b shows displacement time histories horizontal and vertical relatives to the model base, respectively. These relative displacements where computed in control points 4, 5 and 6 located over the downstream slope. The displacement time histories are very irregular and are plotted by sharp alternate peaks, as a result of the back and forth motion until the end of the excitation. The control point 5 reached the maximum permanent displacements about 0.5 m and 0.25 m in horizontal and vertical axes, respectively.

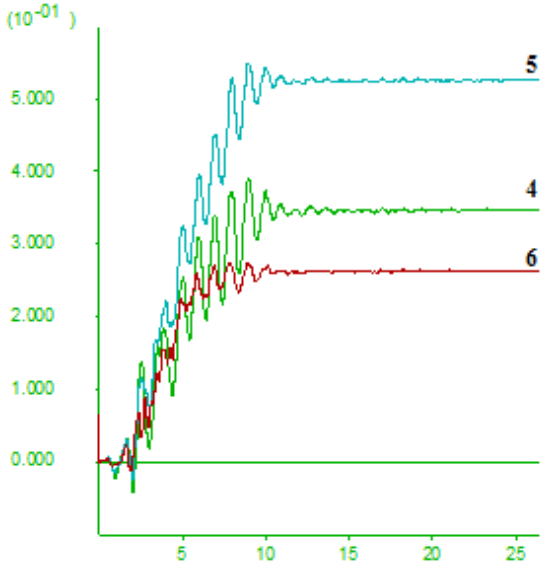

Figure 13a. Horizontal displacements in history points 4; 5 and 6 in meters.

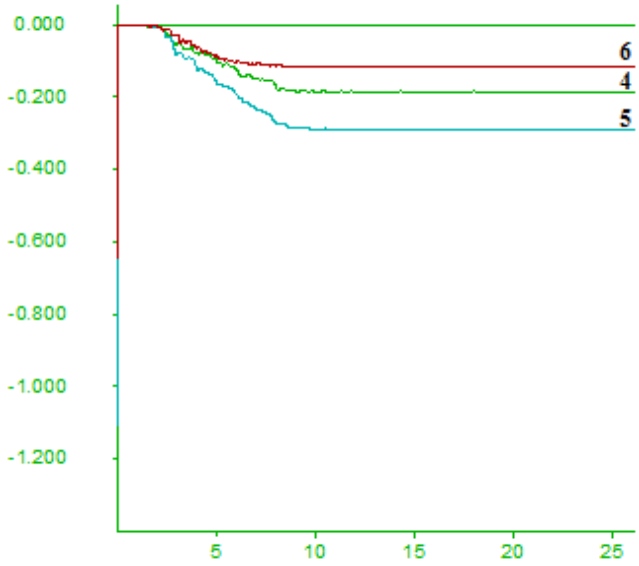

Figure 13b. Vertical displacements in history points 4; 5 and 6 in meters.

Horizontal time history displacements relative to the model base of control points located at the interface region 2, 7 and 8 are presented in Figure 14. The maximum deformation computed in this area reached values below 0.03 m in control points 7 and 8.

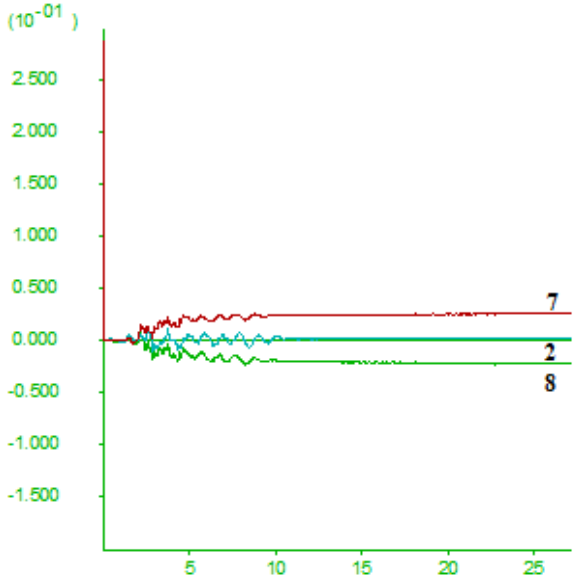

Figure 14. Horizontal displacements in interface history points 2; 7 and 8 in meters.

5 CONCLUSIONS

Using the finite differences method code FLAC, the dynamic behavior in operation-term of a leach pad was modeled and simulated. A built-in Mohr-Coulomb model with stress-level dependent was used for the ore material. From the results of the dynamic analysis it can be concluded that the geostructure will remain safely during an OBE design occurrence, with maximum permanent deformations at the upper region of the downstream benches of about 0.5 m in horizontal and 0.25 m in vertical, permanent deeper deformations in the downstream slope region of about 0.1 m in horizontal and 0.05 m in vertical were registered as well.

The acceleration time history obtained shows an amplification of about 2 times considering the history points located at the top and at the base of the model. The overall deformation pattern of the heap leach facility mainly consists in a slope compaction associated with lateral deformation. The main objective of this stability assessment was to quantify the permanent deformations product of the inertial forces induced by the imposition of an OBE design, the existence of a low permeability soil liner interface (liner system) between the ore stack and soil foundation was not considered for this analysis.

6 REFERENCES

Abrahamson, N. A. 1992. Non-stationary Spectral Matching, Seismological Research Letters 1992; 63(1), 30.

Barton, N., and Kjaernsli, B. 1981. Shear Strength of Rock-Fill, ASCE Journal of the Geotechnical Engineering Division, V. 107(GT7): 873-891.

Barton, N. 2008. Shear Strength of Rock-Fill, Interfaces and Rock Joints, and their Points of Contact in Rock Dump Design, Keynote Address, Rock Dump, Ed. A. Fourie, Perth, Australia.

Coulomb CA. 1976. Sur une application des règles maximis et minimis a quelques problèmes de statique, relatives a l'architecture. Acad Sci Paris Mem Math Phys; 7: 343–382.

Gazetas, G. and Dakoulas, P. 1992. Seismic Analysis and Design of rockfill Dams: State-of-the-Art, Soil Dynamics and Earthquake Engineering 1991; 11: 27-61.

Hancock, J., Watson-Lamprey, J., Abrahamson, N. A., Bommer, J. J., Markatis, A., McCoy, E. and Mendis, R. 2006. An improved method of matching response spectra of recorded earthquake ground motion using wavelets, J. of Earthquake Eng.; 10 (Special Issue 1), 67-89.

ITASCA. 2005. Fast Lagrangian Analysis of Continua (FLAC), Version 5, User's Guide. Itasca Consulting Group, Inc.

Janbu, N. 1963. Soil Compressibility as Determined by Oedometer and Triaxial Tests, European Conference on Soil Mechanics and Foundation Engineering, Wissbaden, Germany, 1: 19-25.

Leps, T.M. 1970. Review of Shear Strength of Rock-Fill, ASCE Journal of the Soil Mechanics andFoundation Engg. Division, V. 96 (SM4), pp. 1159-1170.

Mohr O. 1900. Welche Umstände bedingen die Elastizitätsgrenze und den Bruch eines Materials? Zeit des Ver Deut Ing.; 44: 1524–1530.

Navarro, P., Rivera, M., and Monge, R. 2010. Geología y Metalogenia del Grupo Calipuy (Volcanismo Cenozoico) Segmento Santiago de Chuco, Norte del Perú, Boletín N°28 Serie D; Estudios Regionales; INGEMMET.

Risk Engineering, Inc. 2011, EZ-FRISK™ Online User's Manual, EZ-FRISK™ Version 7.62, Boulder, Colorado.

Seed, H.B. and Idriss, I.M. 1970. Soil Moduli and Damping Factors for Dynamic Response Analysis[R]. U.C. Berkeley, Calif.: EERC.

Seed, H.B., Wong, R.T., Idriss, I.M. et al. 1986. Moduli and Damping Factors for Dynamic Analyses of Cohesionless Soils, Journal of Geotechnical Engineering; 112:11: 1016-1032.